Electronic Supplementary Material (ESI) for CrystEngComm.

Cobalt(II) and Zinc(II)-Coordination Polymers Constructed from Ether-Linked Tetracarboxylic Acid and Isomeric bis(imidazole) linkers: Luminescent based Fe(III) detection in aqueous media

Mürsel Arıcı[a], Yakup Can Dikilitaş[a], Hakan Erer[a] and Okan Zafer Yeşilel[a,*]

[a]Department of Chemistry, Faculty of Science and Letters, Eskişehir Osmangazi University, 26040 Eskişehir, Turkey

Table S1. Selected bond distances and angles for complexes **1**-**2** (Å, º)

Complex 1			
Co1–O1	1.9572 (17)	Co1–N1	2.019 (2)
Co1–O4^{i}	1.9810 (19)	Co1–N4^{ii}	2.055 (2)
O1–Co1–O4^{i}	105.03 (8)	O4^{i}–Co1–N1	123.18 (9)
O1–Co1–N1	112.77 (8)	O4^{i}–Co1–N4^{ii}	113.50 (9)
O1–Co1–N4^{ii}	95.00 (8)	N1–Co1–N4^{ii}	103.92 (9)
Complex 2			
Co1–O1	1.960 (4)	Co1–N3	2.027 (5)
Co1–O3^{i}	2.008 (4)	Co1–N1	2.034 (5)
O1–Co1–O3^{i}	104.35 (19)	O3^{i}–Co1–N3	121.1 (2)
O1–Co1–N3	108.9 (2)	O3^{i}–Co1–N1	115.9 (2)
O1–Co1–N1	94.6 (2)	N3–Co1–N1	108.3 (2)

Table S2. Selected bond distances and angles for complexes **3**-**4** (Å, º)

Complex 3			
Zn1–O1	1.940 (2)	Zn1–N1	2.006 (3)
Zn1–O3^{i}	1.963 (3)	Zn1–N4^{ii}	2.050 (3)
O1–Zn1–O3^{i}	107.88 (11)	O3^{i}–Zn1–N1	118.41 (12)
O1–Zn1–N1	115.47 (12)	O3^{i}–Zn1–N4^{ii}	111.38 (12)
O1–Zn1–N4^{ii}	96.01 (11)	N1–Zn1–N4^{ii}	105.37 (12)
Complex 4			
Zn1–O1	1.939 (4)	Zn1–N3	2.010 (5)
Zn1–O3^{i}	1.969 (4)	Zn1–N1	1.994 (5)
O1–Zn1–O3^{i}	106.3 (2)	N1–Zn1–N3	109.0 (2)
O1–Zn1–N3	96.5 (2)	O3^{i}–Zn1–N3	114.2 (2)
O1–Zn1–N1	111.3 (2)	O3^{i}–Zn1–N1	117.4 (2)

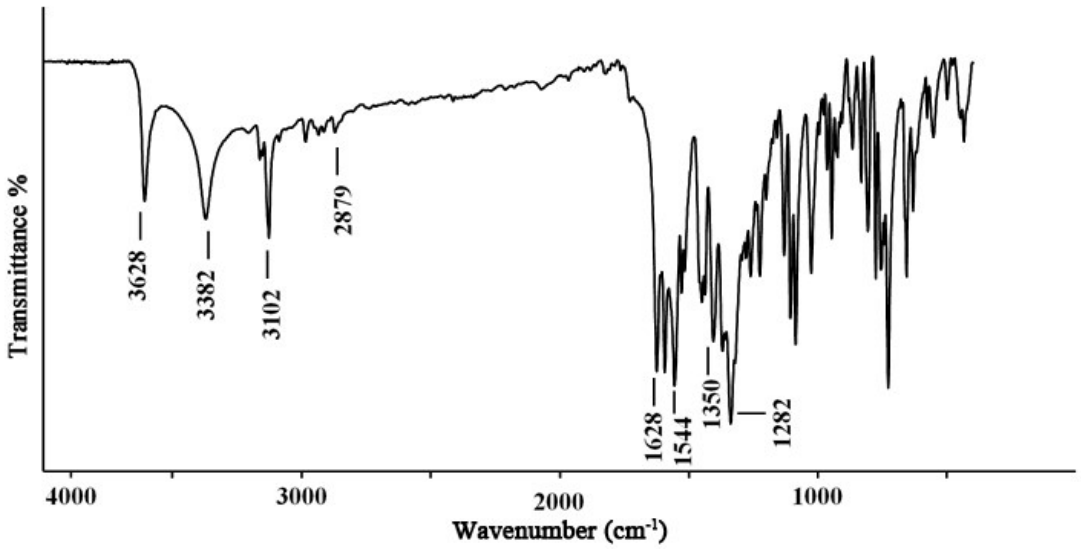

Fig. S1. IR Spectrum for **1**

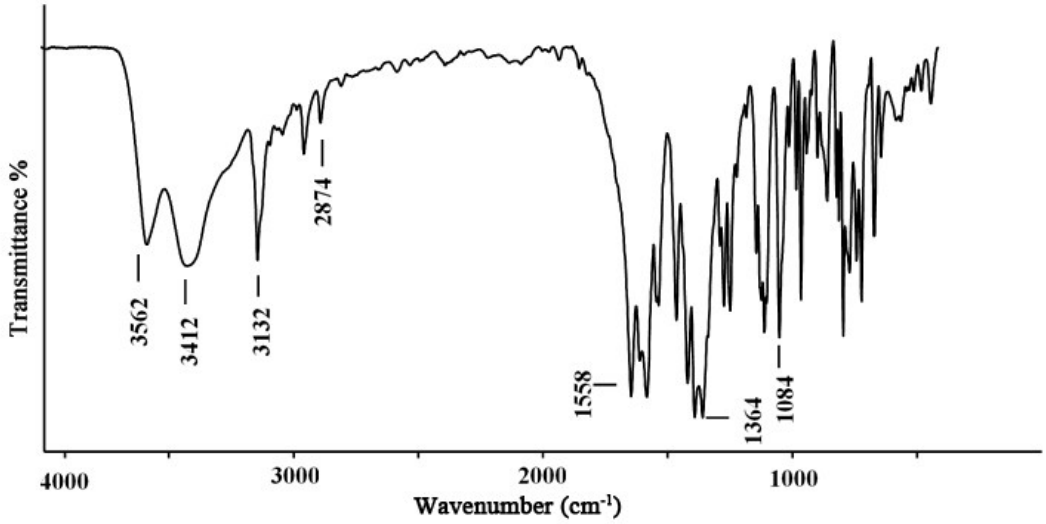

Fig. S2. IR Spectrum for **2**

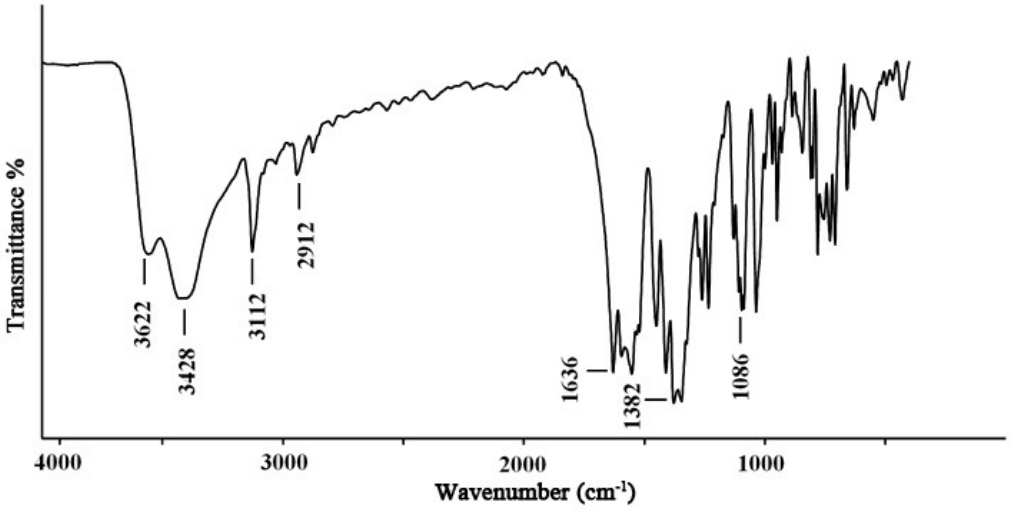

Fig. S3. IR Spectrum for **3**

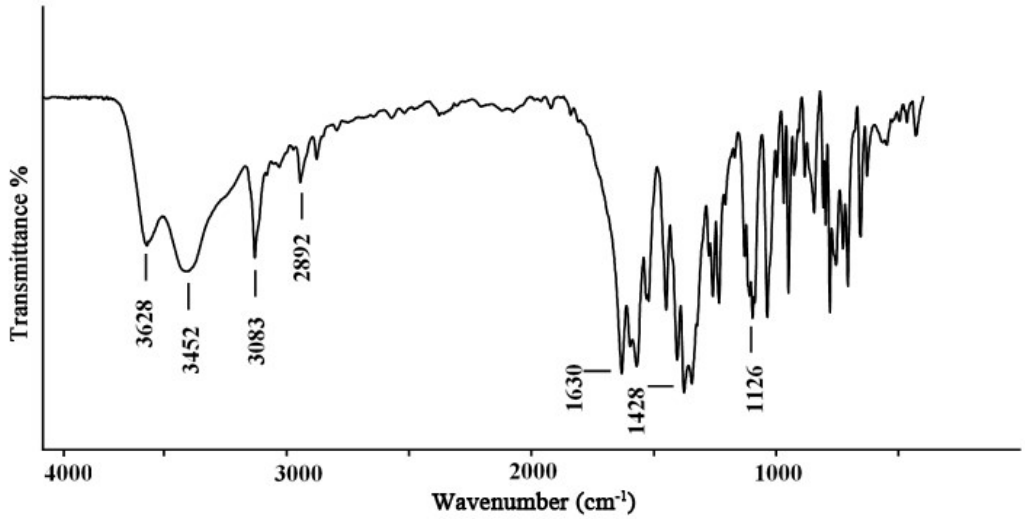

Fig. S4. IR Spectrum for **4**

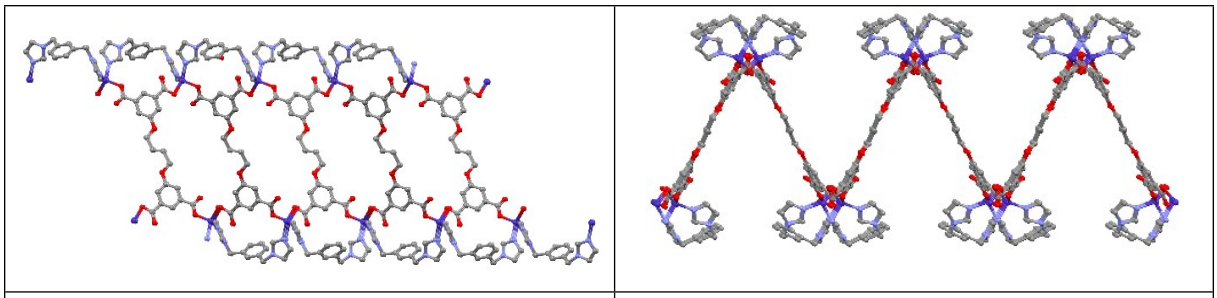

(a) **(b)**

Fig. S5. (a and **b)** A view of undulated 2D coordination sheet of **1** (Symmetry codes

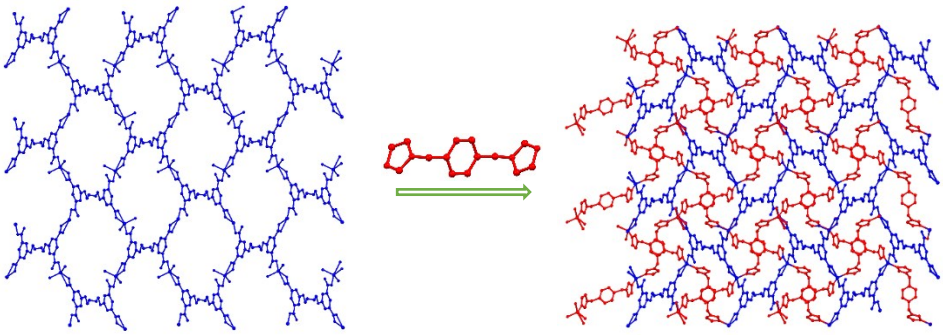

Fig. S6. 2D undulated network and 3D framework of **2**

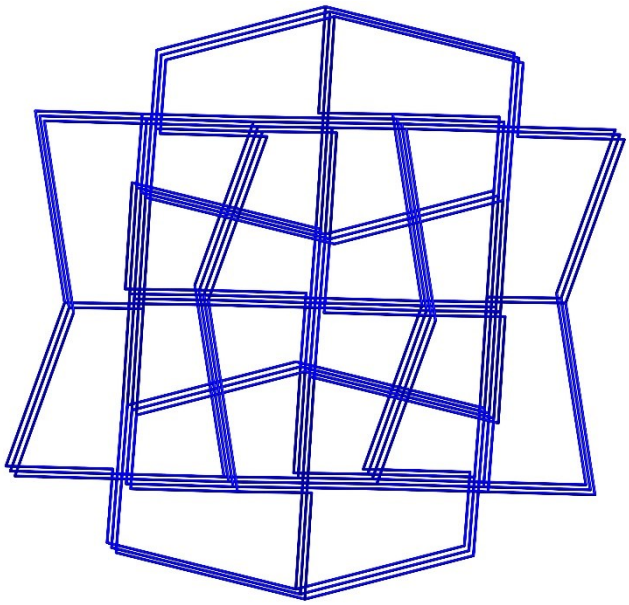

Fig. S7. A view of two nodal 4,4-connected 3D framework of **2**.

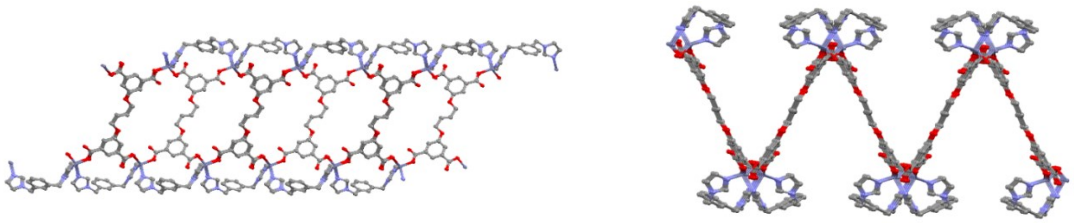

(a) **(b)**

Fig. S8. (a and b) A view of undulated 2D coordination sheet of **3**

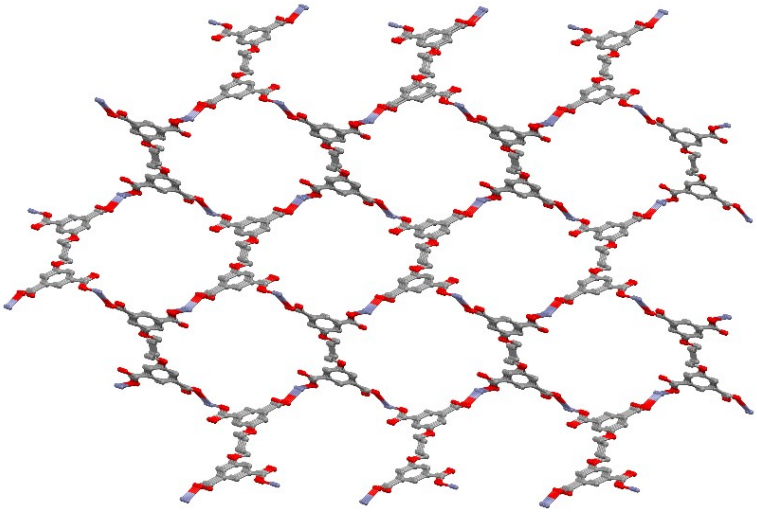

Fig. S9. A view of undulated 2D coordination sheet of **4**

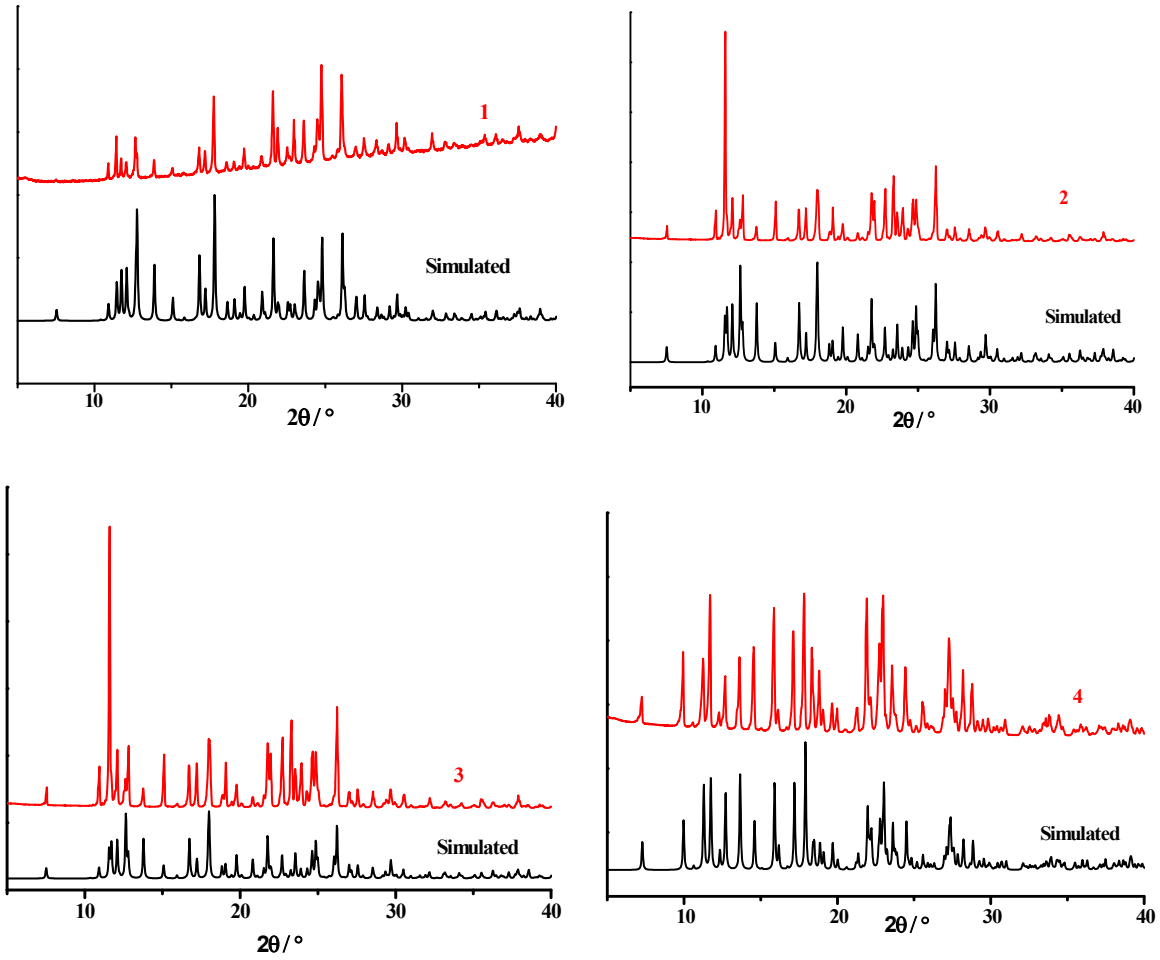

Fig. S10. PXRD patterns of compounds **1-4**

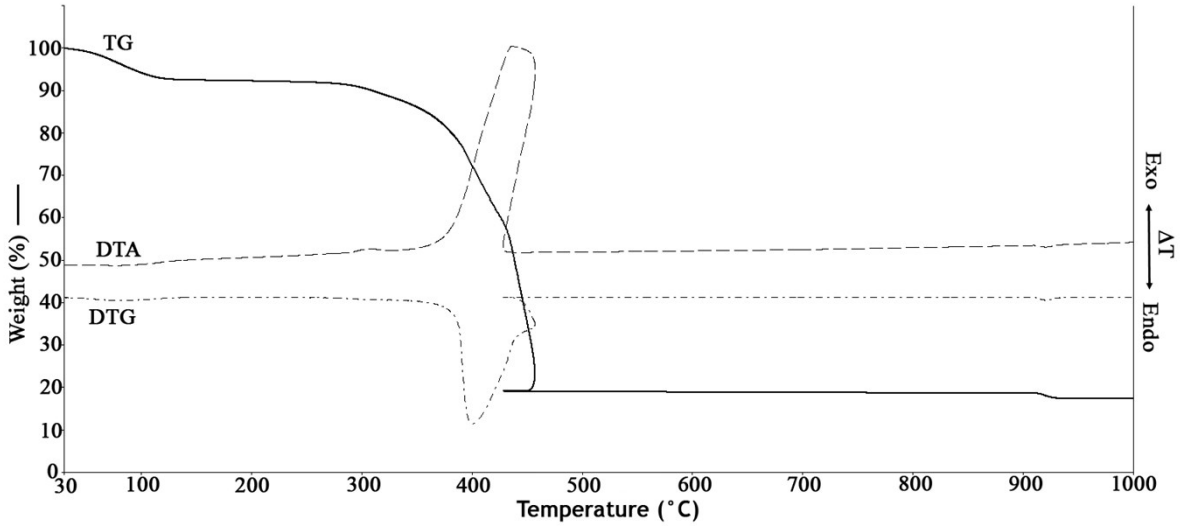

Fig. S11. TG, DTG and DTA curves of compound **1**

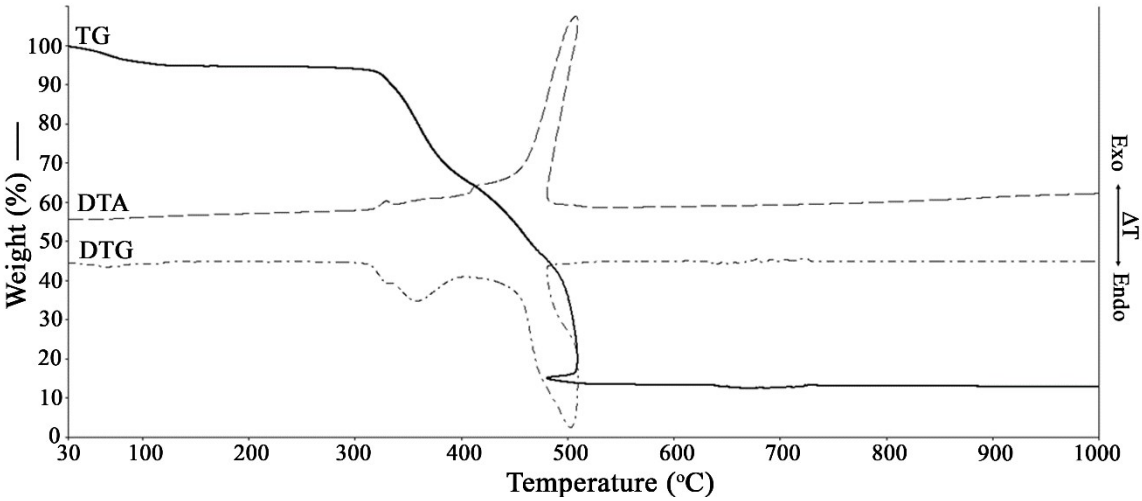

Fig. S12. TG, DTG and DTA curves of compound **2**

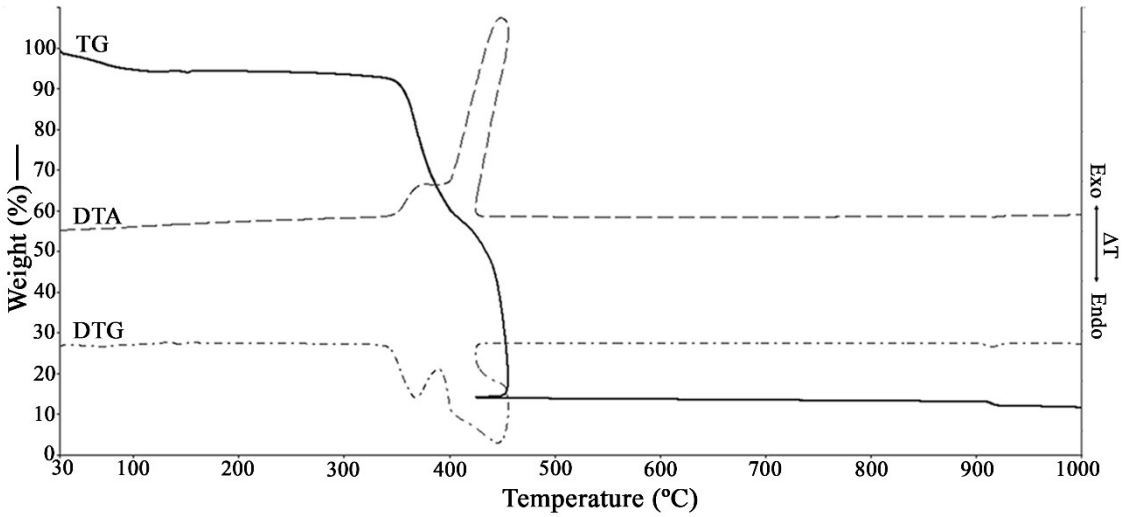

Fig. S13. TG, DTG and DTA curves of compound **3**

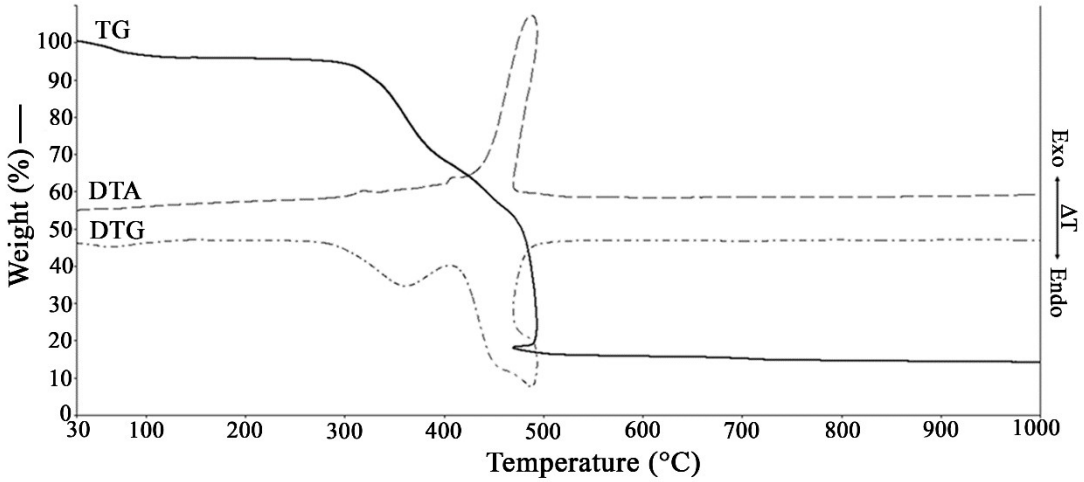

Fig. S14. TG, DTG and DTA curves of compound **4**

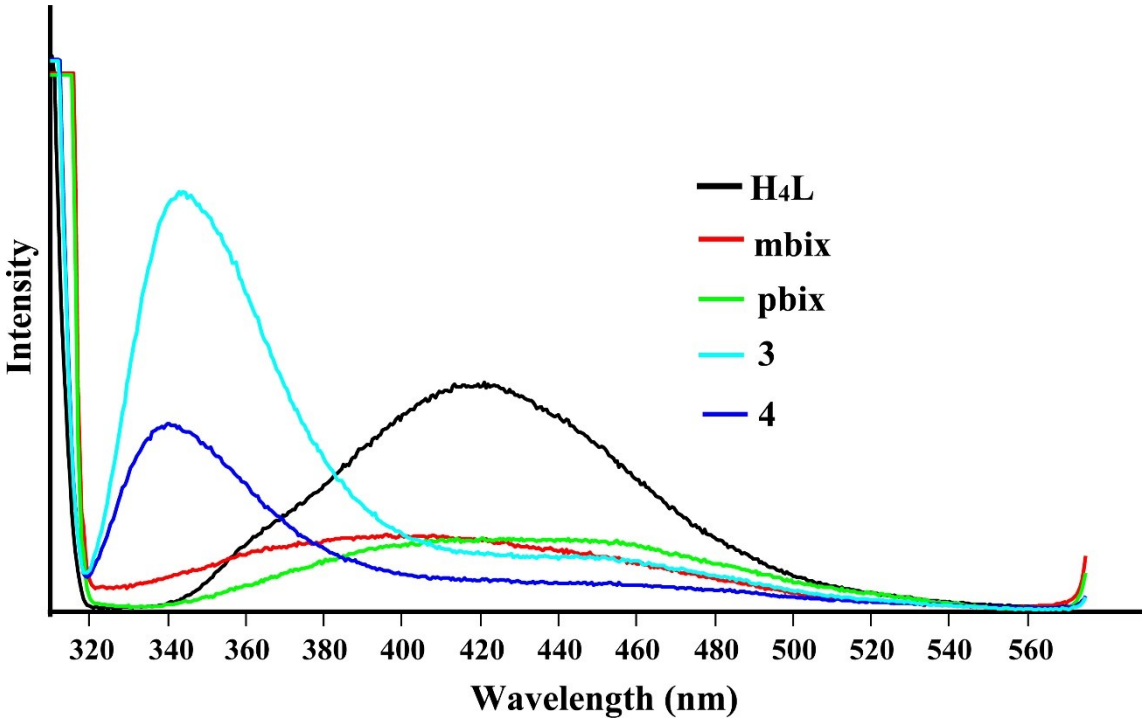

Fig. S15. The solid state spectra of free ligands and compounds **3** and **4**

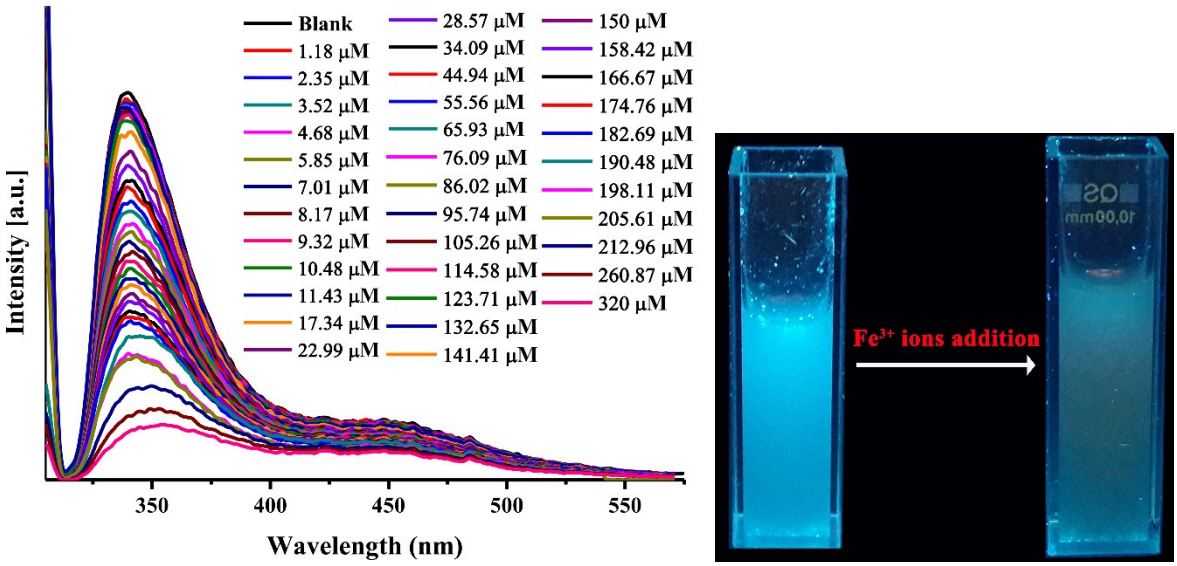

Fig. S16. (a) Emission spectra of **3** dispersed in H_2O upon incremental addition of Fe^{3+} ions (10^{-3} M, 20μL) **(b)** The photographs of **3** dispersed in H_2O before and after the addition of Fe^{3+} ions under UV-light

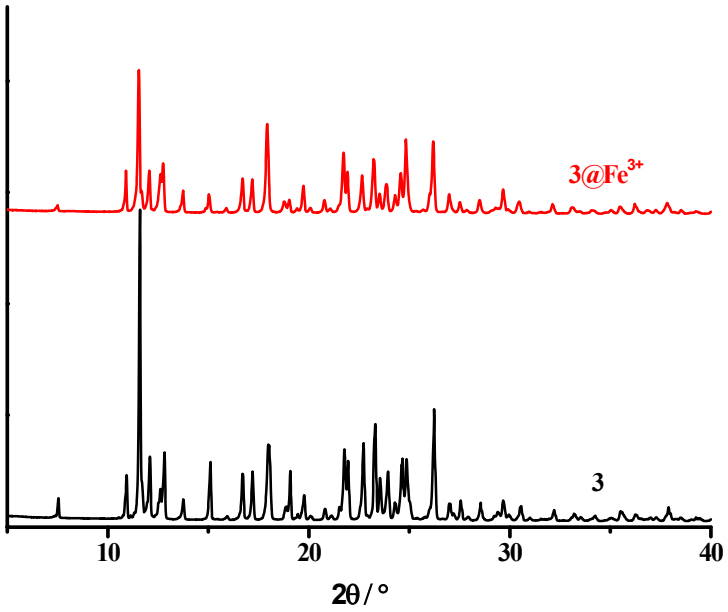

Fig. S17. PXRD patterns of compound **3** before and after the detection of Fe^{3+} ions

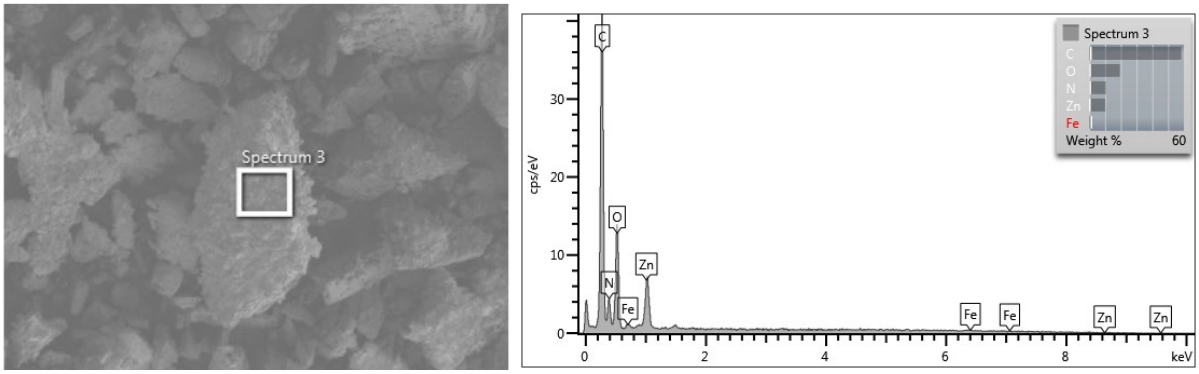

Fig. S18. SEM image and EDX result of recovered compound 3 after immersed in Fe^{3+} solution

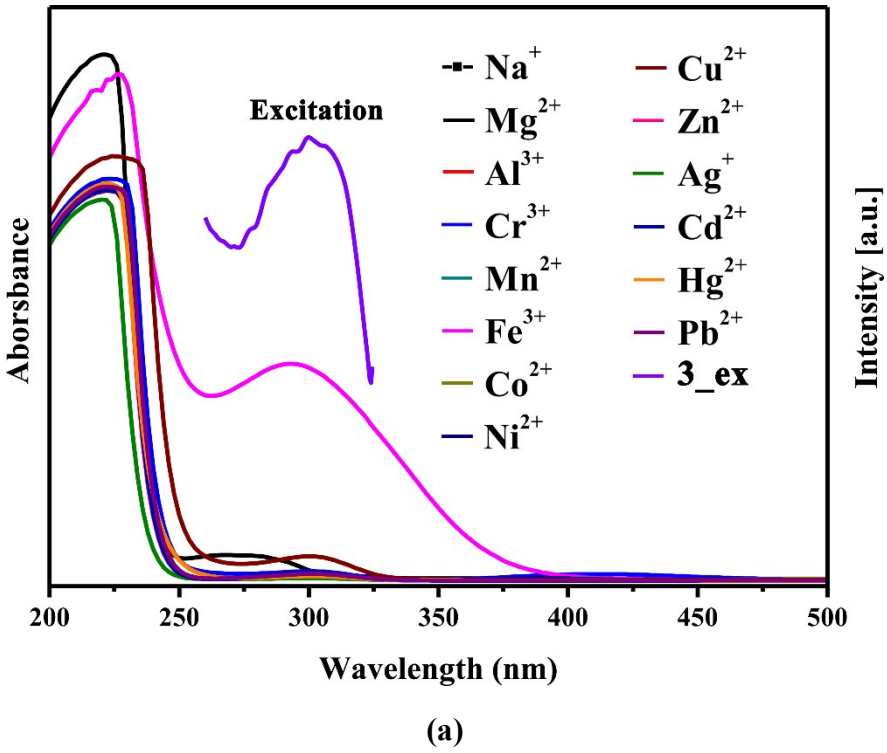

(a)

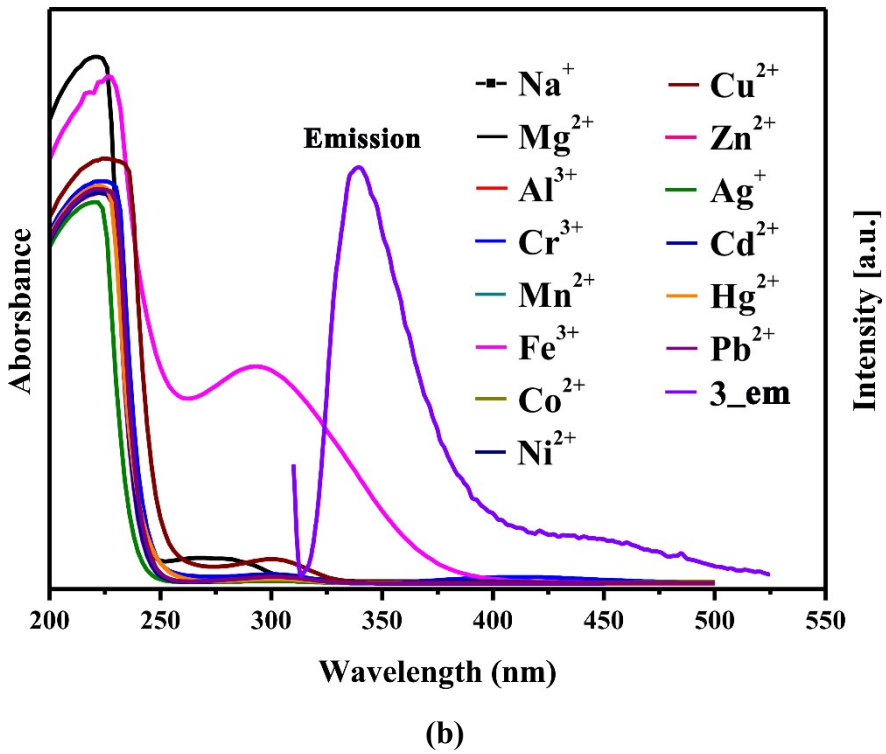

(b)

Fig. S19. (a) Spectral overlap between the absorption spectra of metal ions and the excitation spectrum of compound **3** in H_2O **(b)** Spectral overlap between the absorption spectra of metal ions and the emission spectrum of compound **3** in H_2O